Accuracy of cardiac ablation catheter guidance by means of a single equivalent moving dipole inverse algorithm to identify sites of origin of cardiac electrical activation

Wener Lv[1] · Kichang Lee[2,3,4] · Tatsuya Arai[5] · Conor D. Barrett[3] · Maysun M. Hasan[6] · Alison M. Hayward[7] ·
Robert P. Marini[7] · Maya E. Barley[8] · Anna Galea[9] · Gordon Hirschman[9] · Antonis A. Armoundas[4] · Richard J. Cohen[2]

Abstract

We have developed a system that could potentially be used to identify the site of origin of ventricular tachycardia (VT) and to guide a catheter to that site to deliver radio-frequency ablation therapy. This system employs the Inverse Solution Guidance Algorithm based upon Single Equivalent Moving Dipole (SEMD) localization method. The system was evaluated in *in vivo* swine experiments. Arrays consisting of 9 or 16 bipolar epicardial electrodes and an additional mid-myocardial pacing lead were sutured to each ventricle. Focal tachycardia was simulated by applying pacing pulses to each epicardial electrode at multiple pacing rates during breath hold at the end-expiration phase. Surface potentials were recorded from 64 surface electrodes and then analyzed using the SEMD method to localize the position of the pacing electrodes. We found a close correlation between the locations of the pacing electrodes as measured in *computational* and *real spaces*. The reproducibility error of the SEMD estimation of electrode location was 0.21 ± 0.07 cm. The vectors between every pair of bipolar electrodes were computed in *computational and real spaces*. At 120 bpm, the lengths of the vectors in the *computational* and *real space* had a 95% correlation. *Computational space* vectors were used in catheter guidance simulations which showed that this method could reduce the distance between the *real space* locations of the emulated catheter tip and the emulated arrhythmia origin site by approximately 72% with each movement. We have demonstrated the feasibility of using our system to guide a catheter to the site of the emulated VT origin.

Keywords Single equivalent moving dipole · Inverse solution guidance algorithm · Radio-frequency ablation · Catheter guidance

1 Introduction

Prevention of ventricular tachycardia (VT) remains an important medical challenge. VT may cause hemodynamic collapse or degenerate into ventricular fibrillation (VF), potentially causing sudden cardiac death. Implantable cardioverter defibrillators (ICDs) are currently indicated in patients with recurrent VT and do reduce the risk of sudden cardiac death [1, 2]. However, ICDs terminate VT by means of overdrive pacing or delivery of an electrical shock, but ICDs do not prevent

✉ Kichang Lee
kclee@mit.edu

1   Department of Mechanical Engineering, Massachusetts Institute of Technology, Cambridge, MA 02139, USA

2   Institute for Medical Engineering and Science, Massachusetts Institute of Technology, 45 Carleton Street, Room E25-324, Cambridge, MA 02142, USA

3   Cardiac Arrhythmia Service, Massachusetts General Hospital, Boston, MA 02114, USA

4   Cardiovascular Research Center, Massachusetts General Hospital, Boston, MA 02114, USA

5   Department of Aeronautics and Astronautics, Massachusetts Institute of Technology, Cambridge, MA 02139, USA

6   Department of Electrical Engineering and Computer Science, Massachusetts Institute of Technology, Cambridge, MA 02139, USA

7   Division of Comparative Medicine, Massachusetts Institute of Technology, Cambridge, MA 02139, USA

8   Health Sciences and Technology, Massachusetts Institute of Technology, Cambridge, MA 02139, USA

9   Vivonics Inc., Waltham, MA 02451, USA

initiation of the arrhythmia [1, 2]. Hemodynamic collapse from VT may still occur with ICD therapy and the electrical shock delivered by an ICD can be extremely painful [3–6]. Pharmacologic therapy may be used as an adjunct to ICD therapy to reduce the frequency of ventricular arrhythmias but is not as effective as primary therapy.

Radiofrequency (RF) ablation of the site of origin of the VT may prevent the arrhythmia from being initiated. In this procedure, an RF ablation catheter is introduced into the ventricle and RF current is delivered either to the focus that is driving the arrhythmia, as in premature ventricular contraction-induced VF, a critical isthmus as in scar-mediated VT, or the exit site of the focus [7, 8]. While catheter ablation of VT in patients without structural heart disease has a high success rate, catheter ablation of VT in patients with structural heart disease has remained challenging with a lower success rate [9–11].

One challenge is that to identify the site of origin of the arrhythmia, detailed cardiac mapping of the ventricle must be performed. Current mapping techniques are generally suitable for patients with hemodynamically tolerated VT since these methods require that VT be induced and maintained during the mapping procedure [12, 13]. Unfortunately, VT often results in hemodynamic instability and cannot be sustained long enough for mapping to be completed [14]. Although different strategies are available for such cases, including substrate modification or the use of mechanical circulatory support, such approaches are not associated with improved efficacy [15–18]. Although Furniss et al. [19] showed that RF ablation could be used for the treatment of patients with hemodynamically unstable VT, only a subset of patients who would otherwise benefit from ablation therapy undergo the procedure. Cardiac mapping techniques that would not require the patient to be in VT for an extended period could enable RF ablation to be used to treat patients with hemodynamically unstable VT.

In this paper, we use data from an animal model of VT to evaluate the Inverse Solution Guidance Algorithm (ISGA) methodology for guiding an RF ablation catheter. This guidance method analyzes multiple body surface electrical potentials using a Single Equivalent Moving Dipole (SEMD) model of cardiac electrical activity to localize both the exit site of a re-entrant circuit and the tip of the ablation catheter [20–25]. Although the SEMD model is a simplified representation of cardiac electrical activity, it is accurate when the cardiac electrical activity is highly localized, such as when an impulse emerges from the site of origin of the arrhythmia or spreads from the tip of a pacing or ablation catheter.

This method does not take into account detailed anatomical information, variations in tissue conductivity, or boundary effects. Nonetheless, this method enables accurate catheter guidance to the site of origin of the arrhythmia, because the distortions due to any non-idealities similarly affect both the computed locations of the site of origin of the arrhythmia and the

ablation catheter tip. These distortions cancel out when the ablation catheter tip overlaps the origin of the arrhythmia.

The purpose of this study is to investigate the feasibility of using the ISGA method for RF ablation catheter guidance. To test the methodology, we simulated clinical VT by means of rapid pacing via multiple ventricular epicardial electrodes of known location *in vivo* swine model. Each epicardial electrode was stimulated over a range of pacing rates and used to emulate both the site of origin of the arrhythmia and the ablation catheter tip.

2 Methods

2.1 Animal preparation

Ten Yorkshire swine (~ 40 kg) were used. The experimental protocol was approved by the MIT Committee on Animal Care. The swine were pre-anesthetized with Telazol (4 mg/kg), Xylazine (2.2 mg/Kg), and Atropine (0.04 mg/kg) prior to endotracheal intubation. The swine were maintained under anesthesia using positive pressure ventilation (12 breaths/min and a tidal volume of 500 ml) with isoflurane 1–3%.

A micromanometer-tipped pressure sensor (SPC350, Millar Instruments, Houston, TX) was introduced into the right femoral artery through a sheath catheter for blood pressure measurement. At all times, the animals were continually monitored using ECG, pulse oximetry, blood pressure, and body temperature, with all sensors connected to a data acquisition module (TSD104A, Biopac Systems, Santa Barbara, CA). An additional sheath catheter was placed in the right jugular vein for drug and fluid injection purposes. The animal skin was carefully shaved and sanded for attaching body surface potential electrodes.

A standard median sternotomy was performed and the pericardium was opened. A custom-made array of Ag/AgCl bipolar electrodes (0.1 cm of distance between positive and negative electrodes) was sutured to the epicardial surface of each ventricle. The electrodes in the array were aligned and placed on a medical tape so that the relative positions of the electrodes in the array were fixed during the experiment. The spacing between bipolar electrodes #1 and #2 was 0.2 cm. Between all other adjacent bipolar electrodes, the spacing was 1.0 cm. A pair of stainless-steel electrodes (Premium 6500, Medtronic, Inc., Minneapolis, MN) were placed at the apex of each ventricle at the mid-myocardial level and sutured in place. The relative location of the heart within the chest cavity was mapped using the animal's midline. The *real space* X, Y, and Z locations of the bipolar epicardial electrodes in the arrays on the heart were measured manually. The pericardium was then closed. All electrode cables were exteriorized at the midline of the chest and fixed using stay sutures. The chest
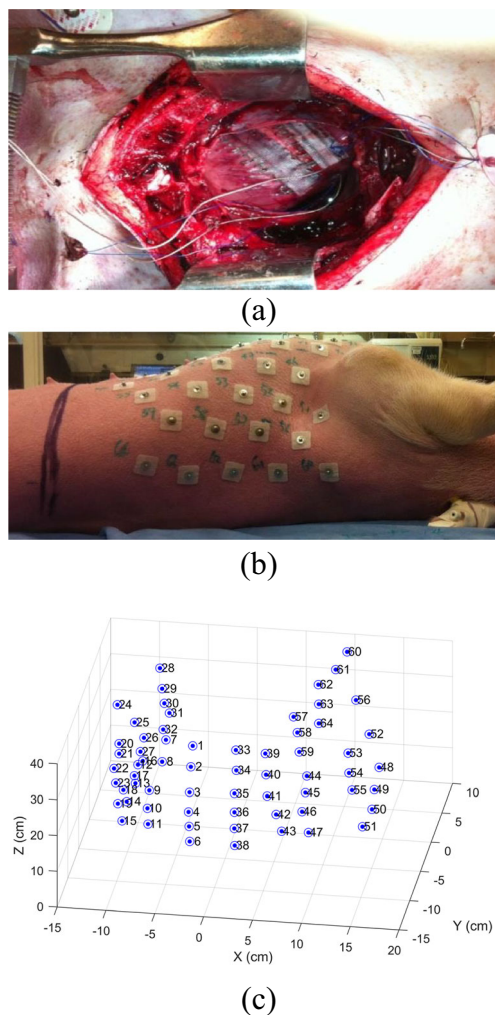
Fig. 1 **a** Picture of an animal heart with an array of epicardial bipolar electrodes on each ventricle, **b** Example of arrangement of body surface ECG electrodes, and **c** example of surface electrode position layout in *computational space*

was closed in layers after air evacuation from the chest cavity. Fig. 1a shows the ventricular electrode placement.

2.2 Experimental protocol

VT was simulated by connecting a stimulus generator delivering pacing spikes (Model STG2008, Multi Channel Systems, Reutlingen, Germany) 1 msec in duration and 3 mA in amplitude to individual epicardial bipolar electrodes to electrically pace the ventricles. Multiple pacing rates were applied, ranging from 120 bpm up to the highest rate resulting in one-to-one ventricular capture (usually 180 bpm).

An array of 64 Ag/AgCl body surface electrodes (A10040–60, Vermed Inc., VT) was placed on the animal's thorax in a symmetrical pattern (Fig. 1b). Swine torso model was estimated using pig's torso length and radius. Surface electrodes were placed, and each electrode's location was mapped on the torso by measuring distance on the X, Y, and Z planes. Visual

confirmation of correct alignment was determined by a computer program displaying 3D layout of electrodes on the swine torso model (Fig. 1c). Using a multichannel bio-potential measurement system (ActiveTwo AD-box, BioSemi, Amsterdam, Netherlands) and a graphical user interface (Labview, National Instrument Corp., Austin, TX), the body surface potentials were collected simultaneously at a sampling rate of 8192 Hz per channel. The collected data segment included approximately 35 cardiac cycles.

To minimize the localization error resulting from chest movement, rocuronium (0.6 mg/kg IV and a maintenance dosage of 0.1 to 0.2 mg/kg every 20 to 30 min) was injected and mechanical respiration was disabled at the end-expiration phase prior to each episode of ventricular pacing. The computed locations of the emulated site of the arrhythmia origin (*target*) and the emulated ablation catheter tip using the ISGA were expressed in *computational space* in contrast to the actual locations of the emulated site of the arrhythmia origins and the emulated ablation catheter tip were expressed in *real (physical) space*. A software program implementing the ISGA was written in Matlab (MathWorks, Natick, MA) and utilized to analyze the collected data. In *computational space*, the locations of the emulated *arrhythmia dipole* and the emulated *catheter dipole* were estimated by analysis of the body surface ECG signals and displayed on the user interface screen.

To evaluate the accuracy of the ISGA method, an array of 16 bipolar electrodes was used to achieve a higher level of spatial resolution in four swine. The space between adjacent bipolar electrodes was 0.5 cm except between bipolar electrodes #1 and #2 where the spacing was 0.2 cm. Each of the bipolar electrodes in each array was paced at heart rates of 120 and 180 bpm.

In order to evaluate the efficacy of the ISGA guidance method, we simulated a catheter guidance experiment *in vivo*. First, the ventricle was paced sequentially at each bipolar electrode and the *computational space* location for each electrode was calculated using the ISGA algorithm. The catheter guidance simulation then considered the bipolar electrodes on a pair-wise basis. The position of the first selected bipolar electrode was used to emulate the location of an ablation catheter tip. The position of the second selected bipolar electrode was used as the location of the origin of the emulated arrhythmia. The location of the second bipolar electrode was, therefore, considered to be the *target*. We then computed locations, trajectories, and orientations of the emulated *arrhythmia dipole* and the emulated *catheter dipole*, as well as a *guidance vector* and *overall distance* between the two dipoles in *computational space*. We then assumed that the emulated catheter was moved from the first electrode to the next electrode by a distance and direction specified by the *guidance vector*. Figure 2 shows the steps of our software explaining the guidance procedure including SEMD calculation.

At the conclusion of the experiment, animals were euthanized with an injection of sodium pentobarbital (100 mg/kg IV). At necropsy, the *real space* coordinates of the epicardial electrodes were confirmed to ensure there were no changes to the original orientation and alignment.

2.3 Inverse solution guidance algorithm

Inverse solution guidance algorithm (ISGA) can be used to localize both (1) the exit point of the site of origin of the arrhythmia and (2) the site of the ablation catheter tip when it is used to pace the ventricles of the heart. ISGA utilizes the SEMD model to analyze the body surface ECG recordings. While the SEMD model can be applied to the entire cardiac cycle, the SEMD model is most accurate when the cardiac electrical activity is highly localized, for example, just as the electrical impulse emerges from the exit point of the site of origin of the VT. ISGA estimates the six dipole parameters (XYZ position coordinates and XYZ components of the dipole moment) at each sample of VT beat to find the trajectory of the single equivalent dipole over the cardiac cycle. The dipole corresponding to the exit site of the re-entrant circuit is selected from an analysis of the trajectory [23, 26].

The earliest activation point (EAP) is selected by analysis of the trajectory of dipole parameters and the ECG signals. The EAP corresponds to the time that the electrical impulse exits from its site of origin. The SEMD at the time point of the EAP is termed the *source dipole*. When the body surface potentials are recorded during VT, the location of the *source dipole* corresponds to the exit point of the site of origin of the VT. When the body surface potentials are recorded during pacing of the ventricles by the RF ablation catheter, the loca-

tion of the *source dipole* corresponds to the site of the bipolar electrode at the catheter tip.

The guidance of the ablation catheter can be achieved by advancing the catheter until the *source dipole* corresponding to the ablation catheter tip is nearly superposed with the *source dipole* corresponding to the site of the origin of the arrhythmia. In the ISGA, for a given dipole location, magnitude, and orientation, the estimated forward potential at the ith body surface electrode, φ_f^i, due to a single dipole is estimated using an infinite volume conductor model (20):

$$\phi_f^i = \frac{\mathbf{p} \cdot (\mathbf{r} - \mathbf{r}_i')}{4\pi g |\mathbf{r} - \mathbf{r}_i'|^3} - \frac{\mathbf{p} \cdot (\mathbf{r} - \mathbf{r}_{ref}')}{4\pi g |\mathbf{r} - \mathbf{r}_{ref}'|^3} \tag{1}$$

where r_i' represents the ith electrode location, r the dipole location, p the dipole moment, g the conductivity of the volume conductor, and r_{ref}' represents the location of the reference electrode.

An objective function, χ^2, describes how well the dipole reproduces the measured voltages:

$$\chi^2 = \sum_{i=1}^{I} \left(\frac{\phi_f^i - \phi_m^i}{\sigma_m^i} \right)^2 \tag{2}$$

where, φ_m^i is the measured potential at the ith electrode, σ_m^i is the standard deviation of the measurement noise in lead i, and I is the number of electrodes.

In the application of the ISGA, voltages are measured using electrodes (64 electrodes in this study) on the volume conductor surface (animal torso in this study), and a brute-force search method is used to find the SEMD parameters that best fit a single time sample of the measured data [27]. The brute-
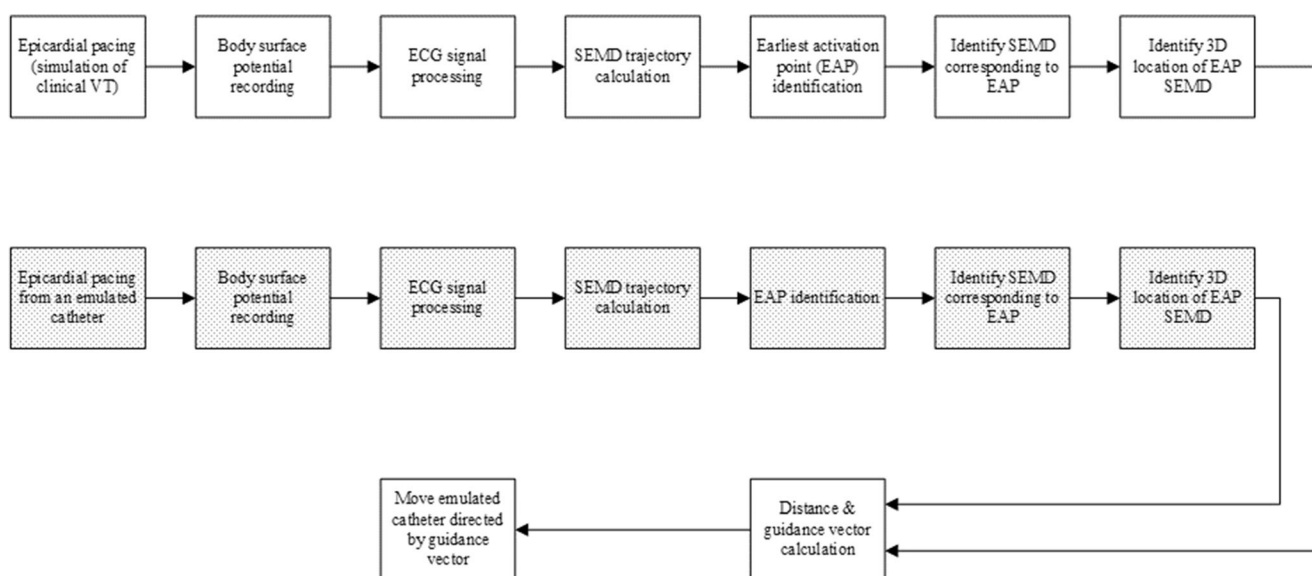

Fig. 2 Basic steps of the guidance procedure including SEMD calculation

force search process commences with the discretization of the volume into cubic volumes (1.5 cm on each side in this study). A dipole is simulated to lie at the center of each cube. Its moment is calculated analytically to optimize the fit to the surface potential data by minimizing the χ^2 function [22]. The dipole, whose location and moment minimize the χ^2 value, is then selected. The cube containing this dipole and its neighboring cubes are discretized into smaller cubes, and the χ^2-minimization procedure is repeated to find the optimal dipole at the new resolution and in the new volume. The process is iterated until the cube dimension is less than a prescribed endpoint (0.5 mm in this study). At this resolution, the dipole whose forward-modeled body surface potentials best reproduce the measured potentials is selected as the SEMD model for that time sample.

In this paper, power line and high-frequency noises, baseline drift, pacing spikes, and other artifacts were removed from the multichannel surface ECG signals after recording. ECG waveforms in all channels were then synchronized and the median waveform of 35 beats for each channel was computed. The resulting median waveforms were then analyzed using the ISGA to estimate the SEMD trajectory. The trajectory was then analyzed to determine the position of the *source dipole*.

3 Results

3.1 Reproducibility of the ISGA method

In the *computational space* localization of each of the bipolar electrodes, the mean reproducibility error of the ISGA method was less than 0.25 cm (0.23 ± 0.06 cm for the right ventricle and 0.17 ± 0.06 cm for the left ventricle with a pacing rate at 120 bpm; the mean error was 0.20 ± 0.12 cm for the right ventricle and 0.21 ± 0.08 cm for the left ventricle with a pacing rate of 180 bpm). Averaged over both heart rates, the reproducibility error was 0.21 ± 0.07 cm, with a maximum of 0.42 cm.

3.2 Correlation of image space and real space localization

In each experiment for each pacing rate, the vector difference in position was calculated between each pair of bipolar electrodes in both *computational space* and *real space*. For each vector component—X, Y, and Z, we calculated the slope of the regression line between *computational* and *real space* and the associated correlation coefficient. We computed these results separately for data from the right and left ventricles. Figure 2a–d display, for one example, at a pacing rate of 120 bpm for the left ventricular electrodes, a sample regression line for each vector component and for the vector length.

Tables 1 and 2 display the correlation coefficients and average slopes for each pacing rate and each ventricle across all experiments.

3.3 Catheter guidance emulation

Catheter guidance emulation was performed for each pair of bipolar electrodes at different heart rates. We then compared the *real space* distance between the emulated catheter tip and the *target* before and after the emulated catheter underwent the movement specified by the *guidance vector*. In this manner, we could determine whether the ISGA-mediated guidance of the emulated catheter decreased the distance between the emulated catheter tip and the emulated arrhythmia origin (*target*). Figure 2e shows one example plot of the distance between the catheter tip and the *target* after the emulated catheter tip movement versus the distance between the catheter tip and the *target* before the movement. In this example, the slope of 0.31 indicates that on average, each catheter movement reduced the distance between the catheter tip and the *target* by $\sim 70\%$. Table 3 summarizes the data for the left and right ventricles at each pacing rate for different ranges of the initial emulated catheter tip to target distance.

4 Discussion

RF ablation therapies for the treatment of cardiac arrhythmia require a mapping technique(s) to identify the site of origin of the arrhythmia as well as a guidance technique to advance a RF ablation catheter to that site. In this paper, we introduced a new guidance method which involves recording multichannel surface ECG during a brief period of arrhythmia and analyzing surface ECG data to identify the site of origin of the arrhythmia and the catheter tip location. Clinical VT was simulated by means of rapid pacing via multiple ventricular epicardial electrodes of known location *in vivo* swine model. We tested the accuracy of the new method, as well as its capability of identifying the sites of the emulated arrhythmia origin and the emulated catheter tip from the analysis of a short segment

Table 1 Correlation coefficient between *computational space* and *real space* vectors

bpm	Right ventricle				Left ventricle			
	X	Y	Z	Vector length	X	Y	Z	Vector length
120	0.97	0.71	0.92	0.94	0.96	0.65	0.91	0.96
140	0.93	0.71	0.87	0.90	0.94	0.70	0.90	0.93
160	0.90	0.67	0.91	0.90	0.91	0.65	0.86	0.89
180	0.91	0.64	0.79	0.84	0.89	0.59	0.85	0.90
200	0.87	0.59	0.86	0.79	0.83	0.51	0.76	0.83

Table 2 Slope of the regression line between *computational space* and *real space* vectors

bpm	Right ventricle			Left ventricle		
	X	Y	Z	X	Y	Z
120	0.76 ± 0.08	0.61 ± 0.12	0.83 ± 0.13	0.73 ± 0.09	0.61 ± 0.24	0.80 ± 0.06
140	0.79 ± 0.09	0.70 ± 0.28	0.83 ± 0.10	0.71 ± 0.21	0.68 ± 0.31	0.79 ± 0.10
160	0.77 ± 0.11	0.57 ± 0.39	0.87 ± 0.09	0.77 ± 0.13	0.77 ± 0.33	0.79 ± 0.16
180	0.74 ± 0.18	0.51 ± 0.41	0.88 ± 0.15	0.77 ± 0.16	0.61 ± 0.36	0.84 ± 0.12
200	0.69 ± 0.19	0.54 ± 0.28	0.81 ± 0.16	0.75 ± 0.18	0.59 ± 0.48	0.76 ± 0.19

of multichannel body surface ECG signals. We also demonstrated the ability of guiding an emulated catheter tip to the emulated arrhythmia origin.

In this method, the SEMD model was used to calculate the locations of the emulated origin of the arrhythmia—locations of bipolar electrodes mounted on the epicardial surface of the heart [20–25]. Each of the bipolar electrodes was used to simulate arrhythmia by pacing the heart with various rates but with the same amplitude.

A recent study showed that the location of SEMD could be identified accurately *in vivo* swine model [25]. In the current study, we made several improvements on epicardial electrode and guidance programs. First, we used a custom-made bipolar electrode which has 2 mm length and 1 mm space between positive and negative electrodes. Second, the median waveform of 35 beats for each channel was computed and used. Third, we added referential electrode location information to calculate the estimated forward potential of the body surface electrode. The locations of the electrodes calculated in *computational space* were then compared to the locations in *real space*. With the new method, the overall average reproducibility error was 0.21 cm. However, it should be noted that the data were collected over a few hours and therefore incorporate uncertainty from two sources: (1) time-invariant errors, due to measurement noise for instance and (2) error resulting from time-dependent physiologic variation.

The correlation between *real* and *computational space* vectors was greater in the X and Z directions compared with the Y direction (posterior-anterior; Fig. 3). Since no body surface electrodes were placed on the animal's back in this

experiment, the Y direction sensitivity of the ISGA was low. We need further studies to determine the impact of placing more electrodes on the back to improve the Y-axis error. There is a tendency for the correlation coefficient to slightly decrease at higher pacing rates (Table 1); this might be due to the shorter isoelectric period which could increase the errors of identifying the baseline of the ECG or possibly could be caused by functional barriers to conduction which might not be present at lower heart rates.

Other groups have utilized inverse solutions and/or dipole models to identify the site of origin of ventricular activation, which requires sophisticated torso or heart geometry mapping and template matching procedure [28, 29]. However, in our ISGA method, the trajectories and orientation of the dipoles of the emulated arrhythmia origin and the emulated catheter tip were calculated over a cycle of the simulated VT. Using matched trajectory portion and orientation, *guidance vector* and distance were calculated and used for the guidance. The results of simulated catheter guidance suggest that ISGA is capable of guiding the catheter to the *target* position by markedly reducing the distance between the emulated arrhythmia *target* and the emulated catheter tip. For example, when the distance between two locations is greater than 3 cm, the distance between two points is reduced by about 72% with one movement with 120 bpm stimulation (Table 2). This simulation study supports the concept that the ISGA guidance might be used as a simple but effective method to guide a catheter to the target location (i.e., arrhythmia origin).

In addition, we utilized only 12–20 s of VT in our experiments compared with the long duration of sustained VT typically used in current mapping procedures. This further suggests that the ISGA guidance method may be suitable for treating patients who are hemodynamically unstable during VT.

Based on the above analysis and results, this *in vivo* swine simulation study suggests that the ISGA method may be able to efficiently and accurately guide an ablation catheter to the target location by following the *computational space* guidance vector. The method described here may therefore provide several clinical advantages: elimination of the need to sustain VT for prolonged periods and reduction of fluoroscope X-ray exposure and procedure time.
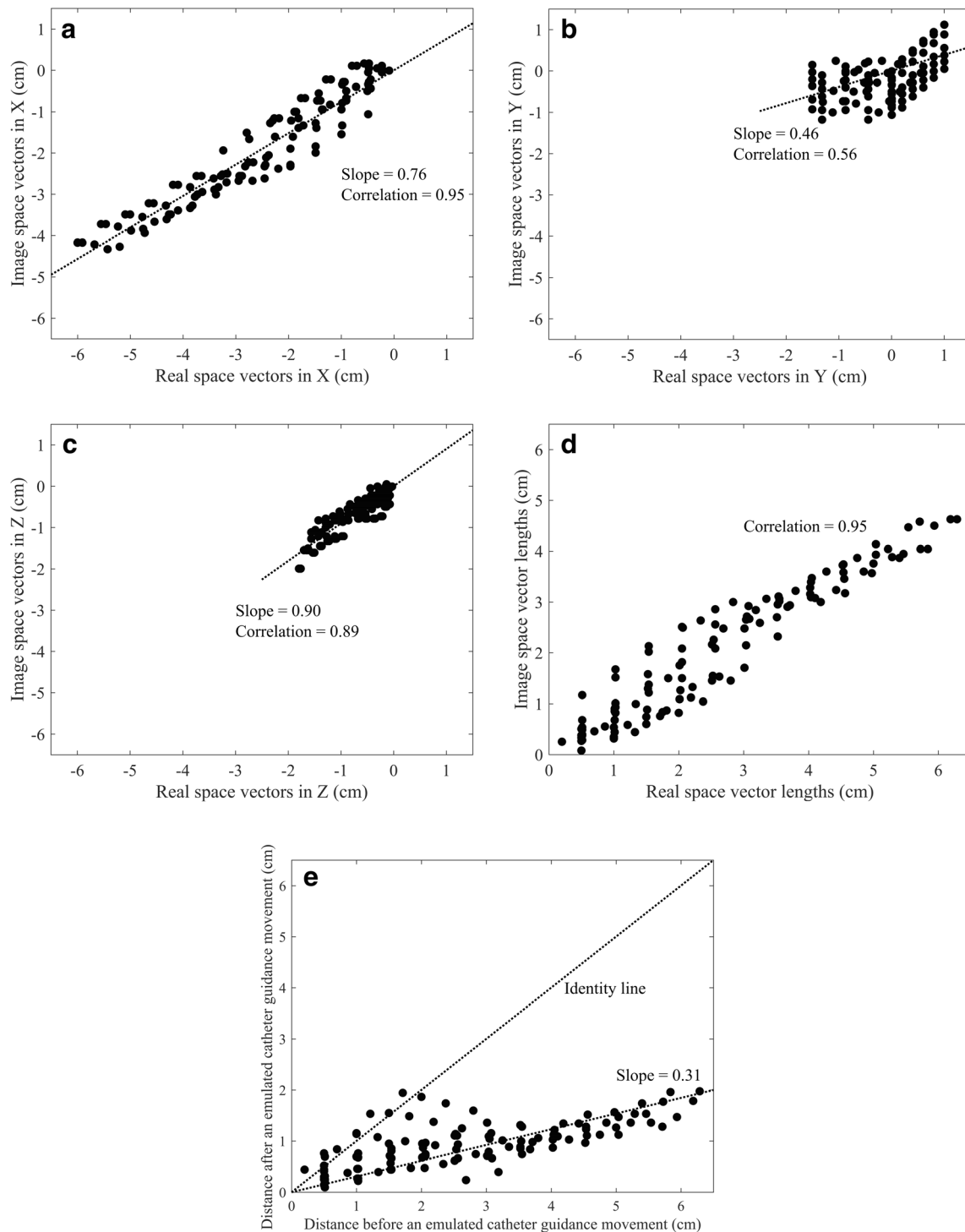
Table 3 Reduction ratio of the distance between the emulated catheter tip and target after one SEMD guidance movement

	Right ventricle		Left ventricle	
Initial distance	< 3 cm	> 3 cm	< 3 cm	> 3 cm
120 bpm	48 ± 25%	72 ± 6%	49 ± 21%	75 ± 13%
140 bpm	37 ± 21%	76 ± 11%	33 ± 20%	85 ± 6%
160 bpm	39 ± 24%	61 ± 12%	39 ± 23%	82 ± 7%
180 bpm	29 ± 18%	70 ± 15%	35 ± 24%	77 ± 9%
200 bpm	33 ± 22%	52 ± 22%	34 ± 23%	61 ± 16%

Fig. 3 Sample plot of vectors between every bipolar pacing electrodes in **a** X-, **b** Y-, **c** Z-dimension, **d** vector length, and **e** the effect of the emulated guidance. Data were collected from 120 bpm left ventricular epicardial electrode pacing experiment utilizing the 16 bipolar electrode arrays. (X—swine's left to right; Y—swine's back to front chest; Z—swine's tail to head)

4.1 Limitations

This study was designed to simulate VT using pacing each bipolar electrode at known electrode locations, and only monomorphic VT was simulated. We did not test the potential suitability of the method for treating polymorphic VT. We studied pigs without structural heart disease which is commonly present in patients with VT. In addition, for this study, we used a paralytic drug (rocuronium) to minimize the localization error resulting from chest movement and collected

ECG data at the end-expiration phase while pacing the heart. It might be possible that the chest movement due to respiration could introduce some error on our method—for clinical use additional software may be needed to compensate for respiratory artifacts.

The pacing rates used in this study were sufficiently slow that an isoelectric baseline was still present. The method would need to be adapted to deal with rapid VT where no isoelectric baseline is present. This study simulated VT by rapid pacing via multiple ventricular epicardial electrodes. Endocardial pacing was not tested. However, the authors expect that if we apply this method to endocardial pacing (in the case that the VT origin is generated from the endocardial electrode and the catheter tip stimulates the endocardium), similar results will be obtained. The site identified in these studies in which VT is simulated by rapid pacing would likely correspond to the exit site of a re-entrant VT focus—however, confirmation would be required in an actual re-entrant VT animal model. The swine morphology results in inferior results in the Y dimension compared to the X and Z dimensions, as swine have longer front to back space and an oval shape. However, we expect that these results will be less varied in humans as human hearts are closer to the body surface in the X, Y, and Z dimensions. Further studies are warranted to confirm this.

5 Conclusion

In this study, ISGA guidance method based on the SEMD model was tested to identify, in *computational space*, the locations of bipolar electrodes mounted on the epicardial surface of the heart. Pacing of each of the bipolar electrodes was used to simulate VT over a range of heart rates. We found a close correlation between the locations of the electrodes as measured in *computational space* and *real space*. We also performed *in vivo* simulation to test the ISGA method to guide an emulated ablation catheter to the site of the emulated arrhythmia origin.

This study demonstrates the potential feasibility of using the ISGA method to guide an ablation catheter to the exit site of a VT focus. One potential advantage of the ISGA method is that it requires only a few seconds of recorded tachycardia data to locate the arrhythmic focus and only a few seconds of ventricular pacing data to locate the catheter tip. Once the catheter tip has been guided to the exit site of the VT, the operator could choose either to ablate the exit site or use other methods to locate a target within the VT focus. Thus, the ISGA method could potentially provide a means of guiding an ablation catheter to a VT focus without requiring the patient to be in VT for an extensive period, potentially making RF ablation therapy feasible for patients with hemodynamically unstable VT.

References

1. Stevenson WG, John RM. Ventricular arrhythmias in patients with implanted defibrillators. Circulation. 2011;124:e411–4.
2. Yousuf O, Chrispin J, Tomaselli GF, Berger RD. Clinical management and prevention of sudden cardiac death. Circ Res. 2015;116:2020–40.
3. Connolly SJ, Dorian P, Roberts RS, Gent M, Bailin S, Fain ES, et al. Optimal pharmacological therapy in cardioverter defibrillator patients (OPTIC) investigators. Comparison of beta-blockers, amiodarone plus beta-blockers, or sotalol for prevention of shocks from implantable cardioverter defibrillators: the OPTIC Study: a randomized trial. JAMA. 2006;295:165–71.
4. Daubert JP, Zareba W, Cannom DS, McNitt S, Rosero SZ, Wang P, et al. Inappropriate implantable cardioverter-defibrillator shocks in MADIT II: frequency, mechanisms, predictors, and survival impact. J Am Coll Cardiol. 2008;51:1357–65.
5. Serber ER, Sears SF, Sotile RO, Burns JL, Schwartzman DS, Hoyt RH, et al. Sleep quality among patients treated with implantable atrial defibrillation therapy: effect of nocturnal shock delivery and psychological distress. J Cardiovasc Electrophysiol. 2003;14:960–4.
6. van Rees JB, Borleffs CJ, de Bie MK, Stijnen T, van Erven L, Bax JJ, et al. Inappropriate implantable cardioverter-defibrillator shocks: incidence, predictors, and impact on mortality. J Am Coll Cardiol. 2011;57:556–62.
7. Delacretaz E, Stevenson WG. Catheter ablation of ventricular tachycardia in patients with coronary heart disease: part I: mapping. Pacing Clin Electrophysiol. 2001;24:1261–77.
8. Strickberger SA, Man KC, Daoud EG, Goyal R, Brinkman K, Hasse C, et al. A prospective evaluation of catheter ablation of ventricular tachycardia as adjuvant therapy in patients with coronary artery disease and an implantable cardioverter-defibrillator. Circulation. 1997;96:1525–31.
9. Tanawuttiwat T, Nazarian S, Calkins H. The role of catheter ablation in the management of ventricular tachycardia. Eur Heart J. 2016;37:594–609.
10. Dukkipati SR, Choudry S, Koruth JS, Miller MA, Whang W, Reddy VY. Catheter ablation of ventricular tachycardia in structurally normal hearts: indications, strategies, and outcomes-part I. J Am Coll Cardiol. 2017;70:2909–23.
11. Dukkipati SR, Koruth JS, Choudry S, Miller MA, Whang W, Reddy VY. Catheter ablation of ventricular tachycardia in structural heart disease: indications, strategies, and outcomes-part II. J Am Coll Cardiol. 2017;70:2924–41.
12. Stevenson WG, Wilber DJ, Natale A, Jackman WM, Marchlinski FE, Talbert T, et al. Irrigated radiofrequency catheter ablation guided by electroanatomic mapping for recurrent ventricular tachycardia after myocardial infarction: The Multicenter Thermocool Ventricular Tachycardia Ablation Trial. Circulation. 2008;118:2773–82.
13. Cuculich PS, Schill MR, Kashani R, Mutic S, Lang A, Cooper D, et al. Noninvasive cardiac radiation for ablation of ventricular tachycardia. N Engl J Med. 2017;377:2325–36.
14. Stevenson WG, Friedman PL, Kocovic D, Sager PT, Saxon LA, Pavri B. Radiofrequency catheter ablation of ventricular tachycardia after myocardial infarction. Circulation. 1998;98:308–14.
15. Miller MA, Dukkipati SR, Mittnacht AJ, Chinitz JS, Belliveau L, Koruth JS, et al. Activation and entrainment mapping of hemodynamically unstable ventricular tachycardia using a percutaneous left ventricular assist device. J Am Coll Cardiol. 2011;58:1363–71.

16. Josephson ME, Anter E. Substrate mapping for ventricular tachycardia: assumptions and misconceptions. JACC Clin Electrophysiol. 2015;1:341–52.

17. Sacher F, Lim HS, Derval N, Denis A, Berte B, Yamashita S, et al. Substrate mapping and ablation for ventricular tachycardia: the LAVA approach. J Cardiovasc Electrophysiol. 2015;26:464–71.

18. Komatsu Y. Substrate-based approach for ventricular tachycardia in structural heart disease: tips for mapping and ablation. J Arrhythm. 2014;30:272–82.

19. Furniss S, Anil-Kumar R, Bourke JP, Behulova R, Simeonidou E. Radiofrequency ablation of haemodynamically unstable ventricular tachycardia after myocardial infarction. Heart. 2000;84:648–52.

20. Armoundas AA, Feldman AB, Mukkamala R, Cohen RJ. A single equivalent moving dipole model: an efficient approach for localizing sites of origin of ventricular electrical activation. Ann Biomed Eng. 2003;31:564–76.

21. Armoundas AA, Feldman AB, Mukkamala R, He B, Mullen TJ, Belk PA, et al. Statistical accuracy of a moving equivalent dipole method to identify sites of origin of cardiac electrical activation. IEEE Trans Biomed Eng. 2003;50:1360–70.

22. Barley ME, Armoundas AA, Cohen RJ. A method for guiding ablation catheters to arrhythmogenic sites using body surface electrocardiographic signals. IEEE Trans Biomed Eng. 2009;56:810–9.

23. Fukuoka Y, Oostendorp TF, Sherman DA, Armoundas AA. Applicability of the single equivalent moving dipole model in an infinite homogeneous medium to identify cardiac electrical sources: a computer simulation study in a realistic anatomic geometry torso model. IEEE Trans Biomed Eng. 2006;53:2436–44.

24. Lee K, Lv W, Ter-Ovanesyan E, Barley ME, Voysey GE, Galea AM, et al. Cardiac ablation catheter guidance by means of a single equivalent moving dipole inverse algorithm. Pacing Clin Electrophysiol. 2013;36:811–22.

25. Sohn K, Lv W, Lee K, Galea A, Hirschman G, Barrett C, et al. A method to noninvasively identify cardiac bioelectrical sources. Pacing Clin Electrophysiol. 2014;37:1038–50.

26. Barley M. Bioelectrical strategies for image-guided therapies. Harvard-MIT Division of Health Sciences and Technology, Massachusetts Institute of Technology; 2007

27. Rosbury TS. Computer simulation of a novel technique for radiofrequency ablation of ventricular arrhythmias. Department of Electrical Engineering and Computer Science, Massachusetts Institute of Technology; 2006.

28. Sapp JL, Bar-Tal M, Howes AJ, Toma JE, El-Damaty A, Warren JW, et al. Real-time localization of ventricular tachycardia origin from the 12-lead electrocardiogram. JACC Clin Electrophysiol. 2017;3:687–99.

29. Svehlikova J, Teplan M, Tysler M. Geometrical constraint of sources in noninvasive localization of premature ventricular contractions. J Electrocardiol. 2018;51:370–7.